Bifurcations to Periodic and Aperiodic Solutions during Ammonia Oxidation on a Pt Wire

M. Sheintuch* and J. Schmidt

Department of Chemical Engineering, Technion—Israel Institute of Technology, Haifa 32000, Israel
(Received: April 20, 1987; In Final Form: January 6, 1988)

Oscillatory states in ammonia oxidation catalyzed by a platinum wire occur around the stoichiometric ratio of the two reactants. The boundary of the oscillatory domain is identified as a soft (Hopf) bifurcation at low temperatures and a hard (global-saddle-node) bifurcation at higher temperatures. We use this information to construct a qualitative model. The oscillatory domain is composed of aperiodic motions interdispersed within bands of multipeak periodic state. Bifurcations in shape of the oscillation occur through one of three routes leading to chaos: period doubling, quasiperiodicity, or intermittency.

Introduction

Singularity theory provides us with a powerful tool for classification and organization of experimental observations and their comparison with analytical results. In applying this approach one designs the experiments to identify bifurcation points, points of transition in characteristic behavior, by sweeping a parameter like feed concentration or temperature. The loci of these bifurcations are traced then by changing another operating condition. The resulting bifurcation map defines the domains of existence of each behavior, or their coexistence, in similarity to phase-transition diagrams. Like the latter, bifurcation maps can be employed for determining design and control procedure, for modeling the behavior, and for comparing various systems in the absence of a model. Thus, the map itself can be viewed as a qualitative model.

Bifurcation maps have been experimentally traced for many catalytic reactions showing steady-state multiplicity.[1,2] Singular points in this case are either ignition or extinction points, their identification is relatively simple, and their modeling usually requires algebraic equations. The loci of these limit points can be traced to their coalescence at a cusp point. The multiplicity bifurcation set is a property of the steady-state model, and oscillatory states which are common to catalytic reactions are usually substituted by time averages in such an analysis.

Maps of dynamic bifurcations were experimentally traced for the Belousov-Zhabotinskii (B-Z) reaction[3,4] and electrochemical reactions.[5] Dynamic bifurcation maps of cool-flame and catalytic oscillations[6,7] were constructed from one-dimensional bifurcation diagrams.[8,9] Such a posteriori construction, however, cannot resolve the ambiguities in the identification process. Four modes of bifurcation to simple oscillation are possible. They can be accounted for by two ordinary differential equations, and the identification of bifurcation is based on the existence or absence of the following three features: continuity of amplitudes, hysteresis, and infinity of the period. Ambiguity in the identification is due to insufficient resolution of experiments near the boundary.

Oscillations in ammonia oxidation, as in most catalytic reactions,[10,11] are of complex shape for most of the oscillatory domain. Their shape is usually classified as multipeak periodic, quasiperiodic (of two characteristic frequencies), or chaotic. Classification of experimental observations and the determination of transition between them cannot always be determined from inspection of time traces and require the employment of more elaborate tests.

Three major routes are generally accepted to account for transitions in shape of oscillations,[12] but the theory is not complete yet and other (unidentified) transitions were observed experimentally. One-dimensional bifurcation diagrams were mapped and identified for the B-Z reaction and for electrochemical Ni dissolution.[5] Bifurcation diagrams and maps of complex behavior in chemically reacting systems are still rare and difficult to attain for several reasons: (a) a very good reproducibility is required, (b) theoretical guidelines are still missing, and (c) the map itself may be of a complex structure as in the case of the transition from frequency-locked to chaotic states.[13] Maps of complex motion have been determined recently for the B-Z reaction.[14]

This work presents a detailed mapping of dynamic bifurcations of oscillatory solutions during ammonia oxidation catalyzed by an isothermal or a nonisothermal platinum wire. This reaction exhibits a richness of instabilities that is summarized in the next section. Specifically, we review observations of steady-state multiplicity of this reaction to show that they do not interact with the dynamic behavior and can be ignored in the present analysis. We draw the boundaries of oscillatory behavior in the plane of reactant concentrations and identify them in terms of simple oscillations. We then identify the sequence of bifurcations in shape as a parameter is varied and attempt to characterize the structure of the bifurcation map of complex behavior. This work is the first such application of dynamic singularity theory for the design of experiments in a catalytic reaction. Catalytic oscillations have also been observed for oxidation reactions of H_2, CO, and hydrocarbons on transition metals[10,11] (see Razon and Schmitz[11] for a recent review). Previous work typically portrayed one or several bifurcation diagrams without any attempt to identify the bifurcations. Our analysis is aimed at revealing the main features of the underlying kinetic models. The exploitation of the identified dynamic bifurcations to simple oscillations for the construction of a kinetic model was demonstrated by Sheintuch and Luss.[6] We apply this approach here and construct a skeleton model.

The bifurcation map itself may be of importance for design purposes of low-temperature combustion like in the catalytic converter. Pt-catalyzed ammonia oxidation is an important commercial process that is conducted at high concentrations and temperatures; oscillations are known to exist under these conditions as well.

This study also demonstrates that the structure of complex motion in catalytic reactions is as rich as that of the B-Z reaction or of hydrodynamic behavior and it can be analyzed by the same tools.

(1) Harold, M. P.; Luss, D. *Chem. Eng. Sci.* **1985**, *40*, 39-52.
(2) Schmidt, J.; Sheintuch, M. *Chem. Eng. Commun.* **1986**, *46*, 289-309.
(3) Boissonade, Y.; DeKepper, P. *J. Phys. Chem.* **1980**, *84*, 501-506.
(4) Epstein, I. R.; Kustin, K.; DeKepper, P.; Orban, M. *Sci. Am.* **1983**, *248*, 112-123.
(5) Lev, O.; Wolffberg, A.; Sheintuch, M.; Pismen, L. M. *Chem. Eng. Sci.*, in press.
(6) Sheintuch, M.; Luss, D. *Chem. Eng. Sci.* **1987**, *42*, 41-52.
(7) Sheintuch, M.; Luss, D. *Chem. Eng. Sci.* **1987**, *42*, 233-243.
(8) Gray, P.; Griffiths, J. F.; Hasko, S. M.; Mullins, J. R. *Proceedings of the 8th International Symposium of Chemical Reaction Engineering*, Edinburgh, 1984; The Institution of Chemical Engineers, Pergamon: Oxford, U.K.; pp 101-108.
(9) Plitchta, R.; Schmitz, R. A. *Chem. Eng. Commun.* **1979**, *3*, 387-398.
(10) Sheintuch, M. *J. Catal.* **1985**, *96*, 326-346.
(11) Razon, L. F.; Schmitz, R. A. *Catal. Rev. Sci. Eng.* **1986**, *28*, 89-164.
(12) Schuster, H. G. *Deterministic Chaos: An Introduction*; Physik-Verlag: Weinheim, 1984.
(13) Cvitanovic, P.; Jensen, M. H.; Kadanoff, L. P.; Procaccia, I. *Phys. Rev. Lett.* **1985**, *55*, 343-346.
(14) Maselko, J.; Swinney, H. L. *J. Chem. Phys.* **1986**, *85*, 6430-6441.

0022-3654/88/2092-3404$01.50/0

Instabilities in Ammonia Oxidation

Pt-catalyzed ammonia oxidation exhibits two steady-state branches: the lower branch is inactive while states on the upper one are either stable or oscillatory. The upper branch is continuous while the lower is isolated when ammonia concentration is varied at high temperatures. At lower temperatures and oxygen concentrations the roles are reversed and the lower branch becomes continuous. These multiplicity patterns have been observed in various reactors and with different catalyst configurations: a single wire, a single pellet, or a multipellet CSTR.[2] The multiplicity bifurcation set can be accounted for by a model that admits a pitchfork singularity. Inhomogeneous solutions, in the form of a partially ignited wire, may also exist and be stable.[15] The boundaries of various homogeneous and inhomogeneous branches were mapped by Sheintuch and Schmidt.[16] Oscillations were observed around the stoichiometric ratio on all steady-state branches, except for the inactive one.

Previous studies of oscillations employed industrial-type conditions: nonisothermal oxidation on Pt wires and foils at about 10% NH_3 in air. Oscillations under these conditions were reported by Flytzani-Stehanopoulos et al.[17] for ambient temperatures of 25–500 °C. Although the resulting surface temperatures (1000–1200 °C) were significantly higher than those in the present work, the range of concentrations that induce oscillatory solutions extrapolates well with our data. Luss and co-workers[18] observed flickering during oxidation on a Pt wire. They correlated the behavior with hydrodynamic fluctuations and suggested flow instabilities as their origin.

Experimental and Data Analysis Procedures

Ammonia oxidation is catalyzed by a 5–7-cm-long, 0.005-cm-diameter platinum wire (United Mineral and Chemical Co.). In the isothermal mode the wire resistance, and hence average temperature, is maintained at a present value by a (PSI, Model 6100) constant temperature anemometer. In the nonisothermal mode the wire resistance is determined by applying a constant low current. The low current is produced by applying 1–5 V across the catalytic wire in series with a constant 1-kΩ resistor; the measured temperature is unaffected by the applied currents in this range. Feed composition is determined and maintained constant by controlling the flow rates of ammonia, oxygen, and nitrogen by means of (Union Carbide FM 4550) flow controllers. Other pertinent experimental information concerning feed purification and wire activation and regeneration is detailed elsewhere.[2,16]

Time traces presented here are either direct chart recording of filtered voltage output or a digitized unfiltered signal. The voltage signal from the anemometer is proportional to the current required to maintain the wire at a preset resistance. In the former case the signal is filtered by the anemometer with a low pass filter of 10 Hz (24 dB/octave slope). In the latter case the unfiltered signal is sampled and digitized at 10 Hz for 300 s by a (PCI 6380) A/D converter and acquired by a (Commodore MMF 9000) microcomputer. The power spectra of the unfiltered signal shows a peak at 1.2 Hz, significantly above the main frequency of the system (~0.1 Hz). To eliminate these high-frequency fluctuations, the data has been smoothed by replacing the value at each point (V_i) with a weighted average of its next six neighbors ($\sum(4 - |j|)V_{i+j}/16, j = -3, ..., 3$) using a triangular weight distribution. This procedure did not affect the spectra in the range of interest and did not distort the signal.

Time traces are presented as the voltage signal. The rate of heat production (Q) is proportional to ($V_0^2 - V^2$), where V_0 is the anemometer reading in the absence of reaction. Although this transformation is not linear, the amplitude is sufficiently small so that it may be considered linear. Heat generation is the state variable employed when the bifurcation diagrams are plotted. Since two or more reactions are possible in ammonia oxidation, the translation of Q to reaction rate is not possible. The enthalpies associated with the various products, however, are similar.

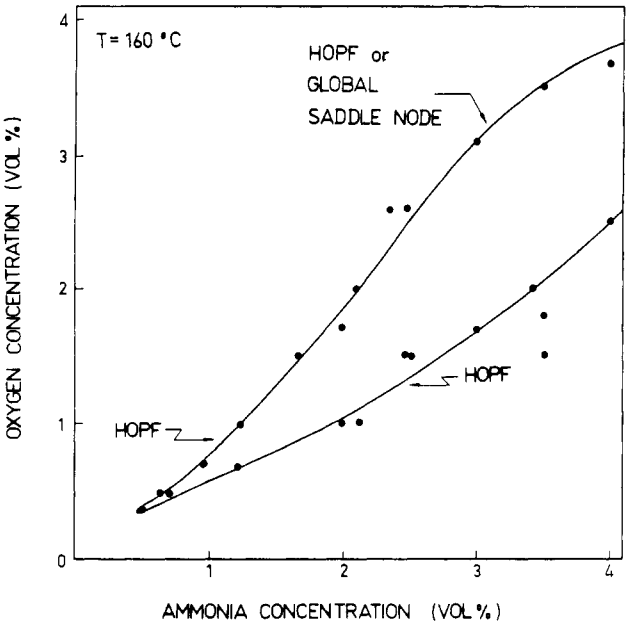

Figure 1. Oscillatory domain at 160 °C; the bifurcation points are denoted by full circles.

Results

(*a*) *Qualitative Observations.* Oscillations exist around the stoichiometric ratio of oxygen to ammonia. In almost all observed oscillatory states this ratio is in the range 0.7–1.1; these values correspond to the stoichiometric ratios of oxygen to ammonia in the reactions that produce N_2 (3/4) or N_2O (1), which are the main products at low temperatures. This observation was made at various temperatures in the range 90–250 °C and with several wires. The bifurcation map at 160 °C is shown in Figure 1.

Oscillations exist only around the active branch. The inactive branch may coexist under these conditions, but the disappearance of oscillations always leads to a stable active state. That applies at high temperatures where the active branch is continuous as well as at low temperatures with a discontinuous upper branch. Thus, we may ignore interaction between the inactive branch and the periodic solutions. At 160 °C the inactive branch is isolated over the whole domain shown in Figure 1. Ammonia concentration at ignition declines with increasing oxygen concentration; i.e., the multiplicity bifurcation set shows a trend opposite to the oscillation boundaries (the ignition line is not shown in Figure 1).

When multiple active states exist, due to inhomogeneity of the wire, then oscillations may exist around several branches in the same range of concentrations. The results shown here were obtained with wires that exhibit only one active state.

In the range of flow velocities employed in this study (~1 cm/s), the linear velocity in the reactor has a minor effect on the oscillations amplitude or shape. This also suggests that the flow controllers do not affect the shape of the oscillations.

To ascertain that the oscillations are not induced by the controlling anemometer, we conducted several nonisothermal experiments and verified that they exist in the same range of concentrations as in the isothermal mode. By switching from isothermal to nonisothermal mode we verified that the two signals are of identical frequencies and similar amplitudes (Figure 2). To compare the amplitudes, the isothermal heat generation is scaled relative to the heat transfer at the set point ($Q_0 = h(T - T_a) = I_0^2R$) and the temperature oscillations are scaled with respect to the wire to ambient temperature gradient. The shape of the two cycles may differ, however; initially the isothermal oscillations are periodic and the temperature fluctuations are aperiodic (Figure

(15) Barelko, V. V.; Kurochka, I. I.; Merzhanov, A. G.; Shkadinskii, K. G. *Chem. Eng. Sci.* **1978**, *33*, 805–811.
(16) Sheintuch, M.; Schmidt, J. *Chem. Eng. Commun.* **1986**, *44*, 33–52.
(17) Flytzani-Stephanopoulos, M.; Schmidt, L. D.; Caretta, R. *J. Catal.* **1980**, *64*, 346–355.
(18) Edwards, W. M.; Zuniga-Chaves, J. E.; Worley, F. L., Jr.; Luss, D. *AIChE J.* **1974**, *20*, 571–581.

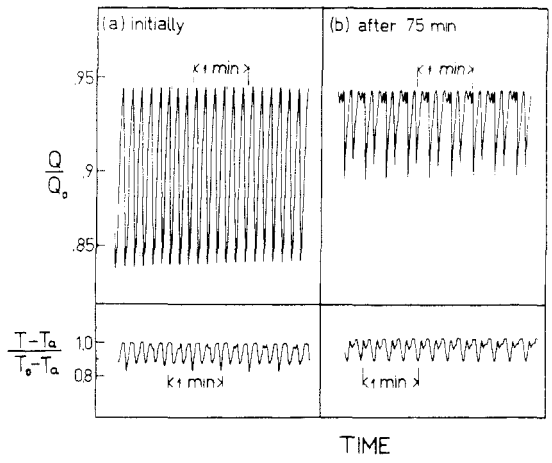

Figure 2. Similarity of isothermal (upper row) and nonisothermal oscillations (lower row); Q_0 is the rate of heat transfer at T_0 = 160 °C, and T_a = 25 °C is the ambient temperature.

2) while the situation is reversed after 75 min.

The slow drift in activity which leads to marked changes in the shape of the oscillations, as noted in Figure 2, is the main obstacle to a detailed mapping of motions. This drift does not affect the nature of the bifurcations to periodic behavior but may alter their position. The sequence of motions observed by increasing a parameter is similar to that observed in the opposite direction usually with a certain drift. We have conducted an extensive study of surface compositions, by Auger analysis, and found that the surface contains high carbon concentrations that could not be removed even by acid etching. Both etched and unetched wires exhibit similar multiplicity patterns and show oscillatory behavior around the stoichiometric reactant ratio. We could not correlate surface composition with any characteristic behavior.

For the reasons outlined above most of the following study into bifurcations was conducted with the same wire over a narrow time period.

(*b*) *Boundaries of the Oscillatory Domain.* We present now observations of transitions from stable to simple periodic solutions, while ignoring the structure of the oscillatory domain. We identify bifurcations observed by changing one reactant's concentrations and searching for their loci when the other concentration is varied.

The lower boundary of the oscillatory domain at 160 °C (Figure 1) is a line of Hopf bifurcations; crossing this line leads to the smooth emergence or disappearance of simple oscillations and their amplitude grows continuously with distance from that line (Figures 3 and 5). The upper boundary is also a smooth Hopf bifurcation at low concentrations. At intermediate concentrations the bifurcation is soft near the boundary but the amplitude grows fast with distance from the bifurcation point. The nature of the boundaries is retained, of course, when oxygen concentration is varied at fixed ammonia concentration.

With increasing concentrations the amplitude growth becomes steeper at the boundaries and the oscillations are of the relaxation type. At 3% NH_3 (Figure 7) the oscillations seem to appear by a hard bifurcation at the right boundary. We checked for and did not detect hysteresis at this boundary. The sequence of time trace in Figure 7 is obtained with decreasing oxygen concentration. Traces a and b, obtained upon crossing the bifurcation set, show the fast establishment of these cycles. At 3.5% O_2 small-amplitude high-frequency oscillations appear in a narrow region near the upper boundary before changing to large-amplitude low-frequency oscillations (Figure 7j,k). Again this transition seems to be discontinuous and without hysteresis. The oscillations near that boundary are of the relaxation type showing upward spikes (Figure 7k). At lower concentration they change into downward spikes before becoming complex in nature.

A discontinuous (hard) bifurcation to periodic behavior may be one of three types:

A saddle-loop (homoclinic) bifurcation occurs when the period orbit collides with a saddle point. The period approaches infinity

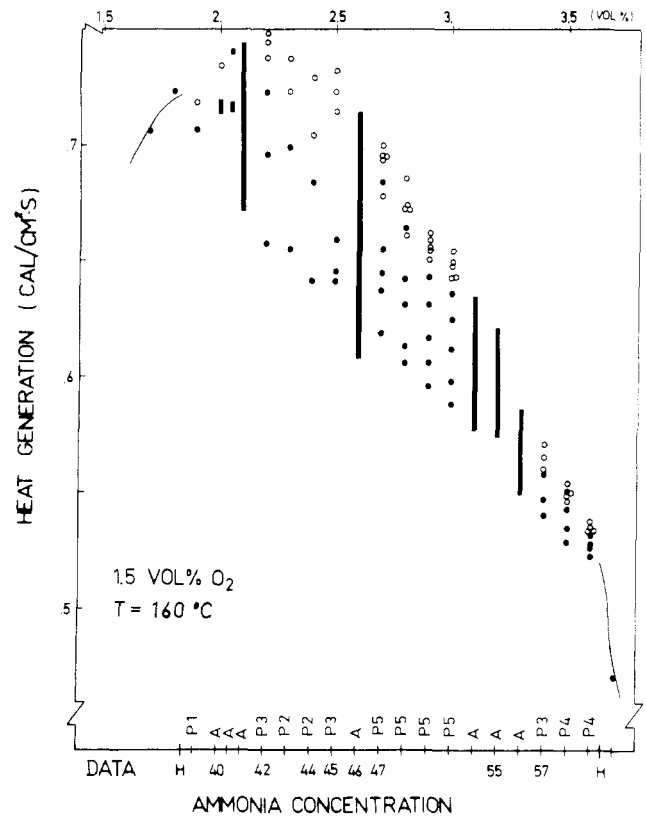

Figure 3. Bifurcation diagram showing heat generation vs ammonia concentration at 1.5 vol % O_2. Upper and lower peaks of periodic state (P*n*) are denoted by open and full circles while aperiodic states (A) are denoted by bands.

at this point, and hysteresis is associated with it.

At a global-saddle-node bifurcation the limit cycle collides with a saddle-node point. The period grows indefinitely at this bifurcation, but the oscillations appear and disappear without hysteresis.

A generalized-Hopf bifurcation is the coalescence of a stable and an unstable limit cycle; the period is finite there and hysteresis is associated with it.

The lack of hysteresis at the upper boundary of Figure 1 indicates that it may be identified as a global saddle node. Another possible explanation, however, is a steep Hopf bifurcation to relaxation oscillations. Analysis of this situation[19] shows that in supercritical bifurcation the amplitude grows moderately in the neighborhood of the Hopf point, followed by a steep increase. In the subcritical Hopf bifurcation to relaxation oscillations the transition is truly discontinuous with a very narrow hysteresis region between the generalized-Hopf and the Hopf points.

To resolve this ambiguity we search for continuity of features in maps of other temperatures. At 176 °C we encountered transition from complex oscillations to a stable steady state which are not intercepted by a region of simple periodicity. These are described in the next section. We conclude there that the bifurcation is global saddle node in nature.

(*c*) *Structure of the Oscillatory Domain.* Most of the oscillatory domain is made of multipeak cycles interdispersed with bands of aperiodic states. A typical bifurcation diagram at low concentrations is shown in Figure 3: the upper (open circles) and lower (closed circles) peaks of multipeak periodic cycles (P*n*) are denoted while aperiodic states (A), i.e., quasiperiodic or chaotic states, are denoted by a band of peaks. To identify the bifurcations in shape of oscillations, it will be necessary to classify the observations.

A sample of time traces, the corresponding power spectra, and time-delayed phase planes is shown in Figure 4. The phase plane is a plot of the actual time series $V(t)$ against the delayed time series $V(t+1\ s)$. The presentation should preserve many of the

(19) Baer, S. M.; Erneux, T. *SIAM J. Appl. Math.* **1986**, *46*, 721–739.

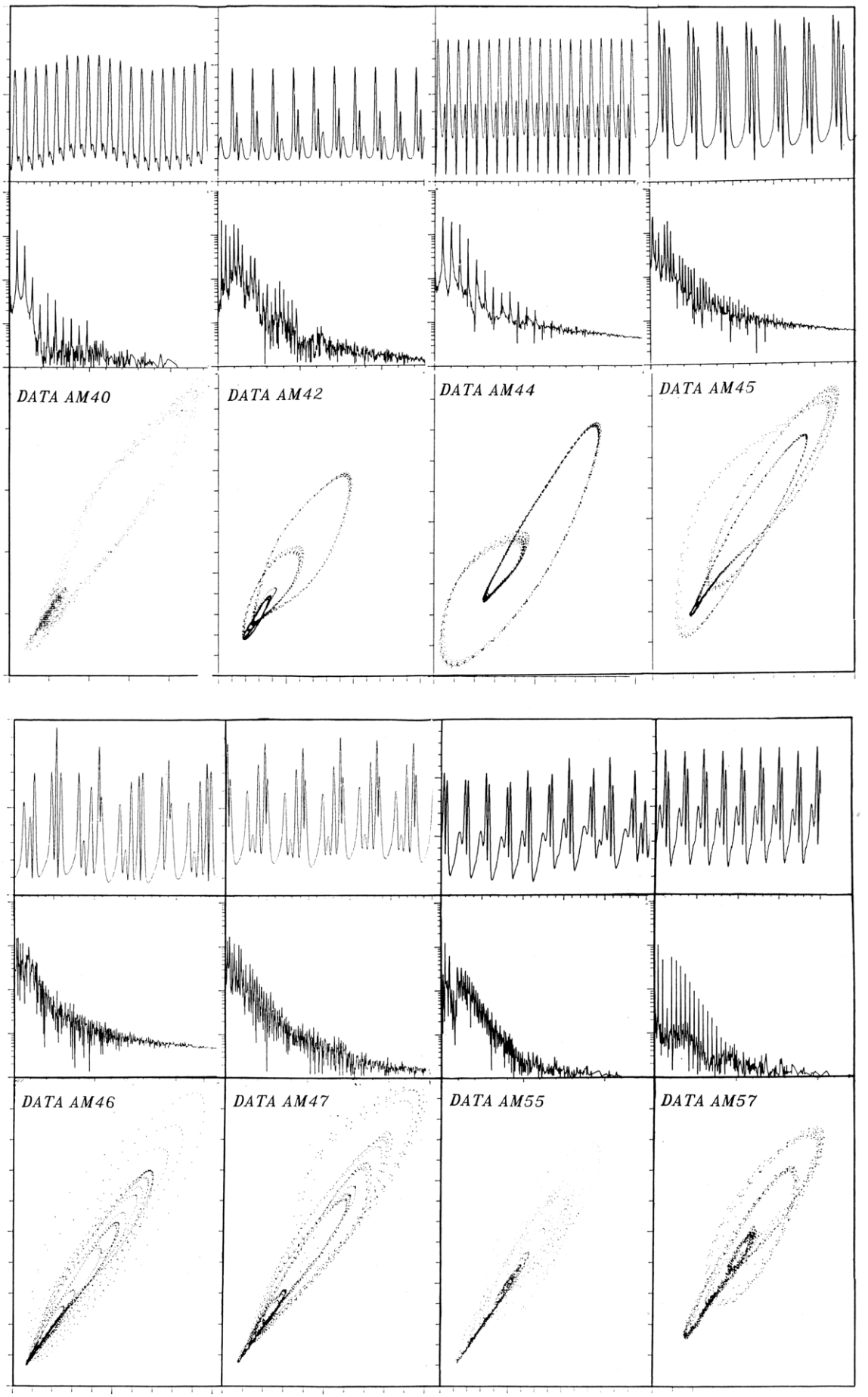

Figure 4. Time traces (upper row, 200 s), power spectra (middle row, 0–1 Hz) and time-delayed phase planes (lower row, 1-s delay) of several states in Figure 3. The voltage scale varies from state to state, but the actual amplitude is shown in Figure 3. Amplitude of the power spectra varies from 10^{-1} to 10^{3}.

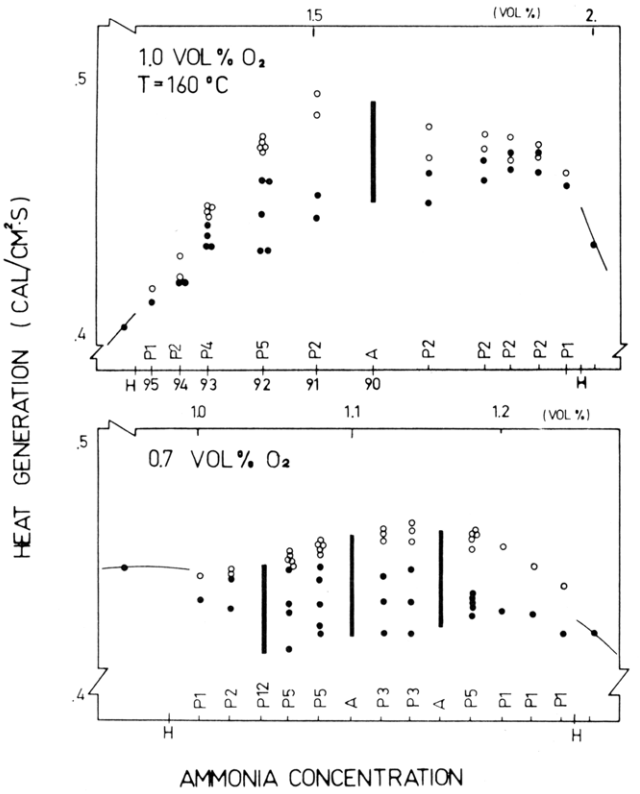

Figure 5. Bifurcation diagrams with varying ammonia concentration at 1% and 0.7% O_2; notation as in Figure 3.

qualities of the actual trajectory. The periodic states P2, P3, and P4 exhibit good reproducibility of the basic cycle, as evident from the phase plane. State P5 (AM 47) shows some scattering, and the aperiodic states tend to fill the whole plane. The power spectra should be helpful in discriminating between quasiperiodic and chaotic states. It also indicates the degree of instrumental noise level; this is relatively low in our case as is evident from states AM 57 and 40, which are close to the Hopf bifurcation point. The spectrum of periodic cycles shows one basic frequency and its harmonics. With increasing number of peaks the basic frequency declines and the spectrum is more densely populated. The oscillations are highly nonlinear and require a large number of terms for their description.

The spectrum of a quasiperiodic state is characterized by two basic frequencies having an irrational ratio and all their linear combinations while a broad-band spectrum characterizes chaos. The spectra of states AM 46 and 55 (Figure 4) do not permit such unambiguous discrimination. Further tests suggest that all the aperiodic states in Figure 3 are quasiperiodic. Computation of the correlation dimension of these states yielded values in the range 1.5–2.0. (Although the correlation dimension is a lower limit to the fractal dimension, the difference between the two measures is usually small; measures of chaos are discussed by Schuster.[12])

The oscillatory domain is narrower at lower ammonia concentrations, but the observed structures at 0.7% and 1% (Figure 5) are similar to that at 1.5%: complex periodic states separated by aperiodic states.

Shape bifurcations usually appear in a sequence. There are three main scenarios that may eventually lead to chaos. We consider them now in order to classify the transitions in Figures 3–6:

The period-doubling scenario consists of consecutive doubling of the period and of the trajectory, ending at a period infinity (infinite number of peaks). A sequence of P1, P2, and P4 states is shown in Figure 6 (AM 95-93), but the adjacent chaos is missing. Studies of one-dimensional maps show that beyond the period-doubling sequence of a simple cycle, periodic states with K peaks per cycle appear and each of these undergoes its own infinite period-doubling sequence. They appear in a certain universal sequence, which does not agree with the data in Figures

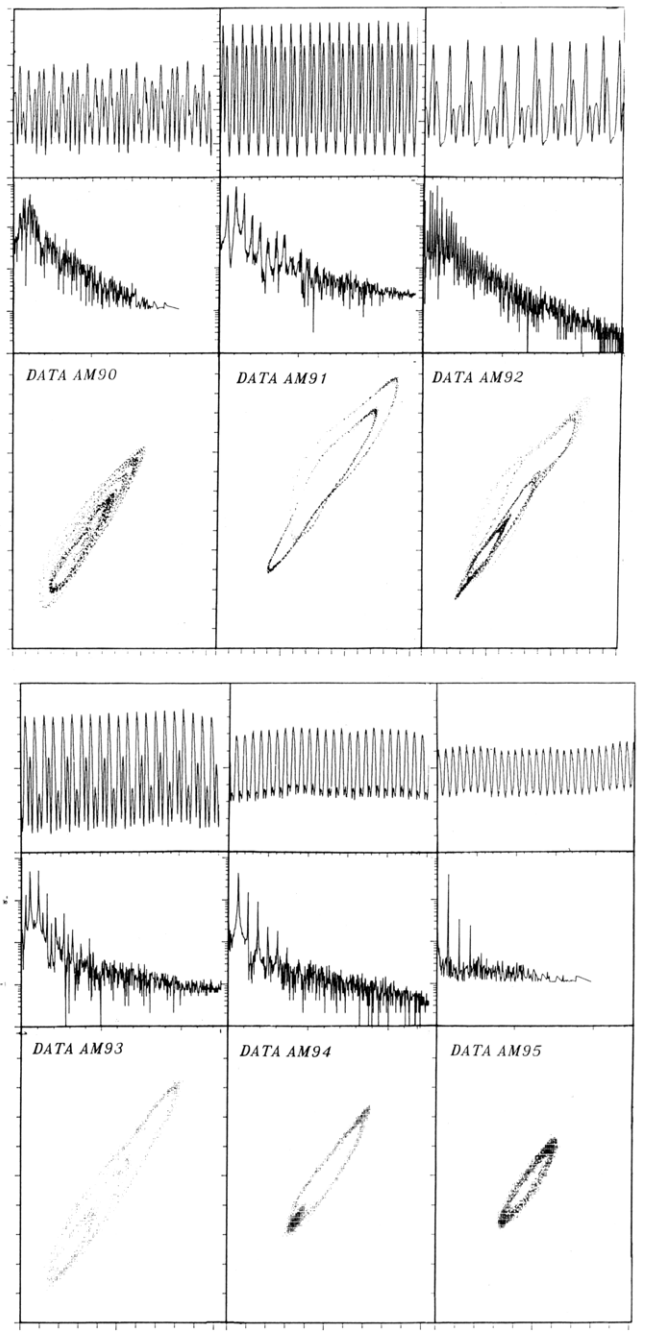

Figure 6. Time traces, power spectra, and time-delayed phase planes of states in Figure 5. Coordinates as in Figure 4; amplitude of spectra varies from 10^{-2} to 10^{2}.

3–6; furthermore, the periodic states should be separated by chaotic states, while the aperiodic states here are mostly quasiperiodic.

In the quasiperiodic transition, two characteristic frequencies give rise to flow on a torus which ultimately breaks in a sequence leading to chaos. This transition is usually intercepted by a region of frequency locking showing periodic behavior with a winding number close to the frequency ratio of the quasiperiodic behavior. A typical bifurcation diagram should include then bands of periodic behavior, with different numbers of peaks, separated by domains of quasiperiodic or chaotic states in agreement with our observations. It is also evident that several bands of aperiodic states were not detected. Such states must separate two periodic cycles of different periodicity (e.g., P4 and P3; Figure 3).

Studies of quasiperiodicity reveal that the frequency-locked (periodic) states form cusp-shaped (Arnold) tongues, in the parameter plane, separated by quasiperiodic or chaotic states. The wider tongues are of small periodicity; P2, P3, P5, etc. The map itself is self-similar in nature, revealing a finer structure with

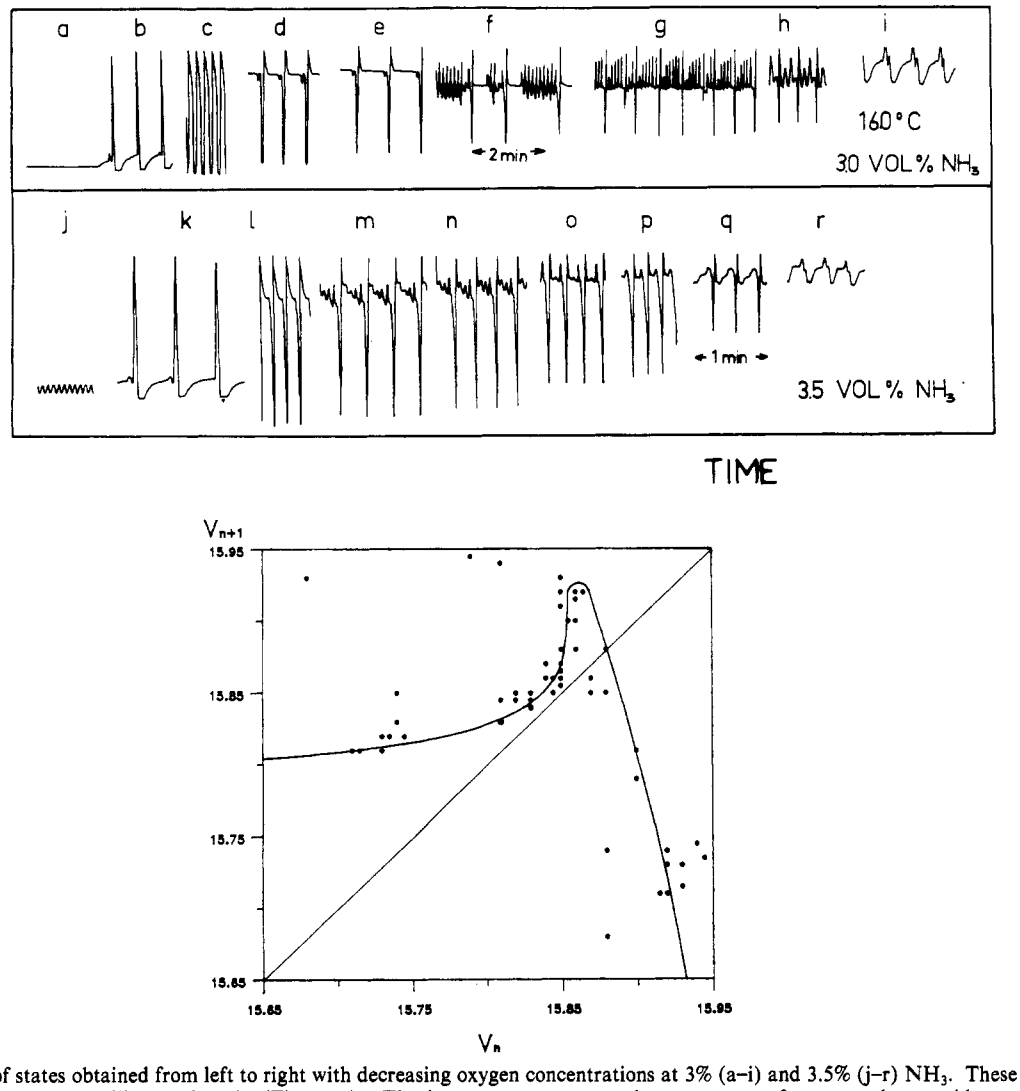

Figure 7. Traces of states obtained from left to right with decreasing oxygen concentrations at 3% (a–i) and 3.5% (j–r) NH_3. These states are almost equally spaced within the oscillatory domain (Figure 1). The lower part, a next-peak return map of state g, shows evidence of intermittence.

increasing magnification. As the tongues grow wider, they overlap and the motion then is chaotic. To test this structure, we have stretched the scale of ammonia concentration in Figure 5 to align the left and right Hopf bifurcations at 0.7% and 1% O_2 and employed similar scaling at 1.5% (Figure 3). The complex periodic states (P2, P3, and P5) are common to these diagrams, and they are interdispersed with aperiodic states, but the various domains are not organized in the same order.

At higher concentrations the oscillations are of the relaxation type, showing a large peak (L) separated by n small ones (s). The structure L + ns is periodic when n is constant; n may vary with operating conditions as in the sequence with 4, 3, 2, and 1 small peaks shown in Figure 7m–p. The aperiodic motion in Figure 7f can be described now by a changing number of small peaks that separate the large ones. Over a sequence of 40 large peaks we could not detect any pattern in the number of small peaks. These shapes are explained in terms of the third scenario leading to chaos.

Intermittency is characterized by bursts of aperiodic oscillations separating periodic regions. Its return map is almost tangential to the diagonal as in Figure 7 (lower part) and thus a large number of (almost periodic) cycles are required to move through the intermediate passage. The trajectory travels then in an aperiodic manner before being reinjected to the periodic region.

The oscillatory states at 176 °C, studied with a different wire than that employed for Figure 1, showed the interaction of two widely different frequencies. The bifurcation diagrams and map are presented in Figure 8. The oscillations disappear via a hard bifurcation at both ends of the oscillatory domain, going through a complex long-period cycle. The transition is not accompanied

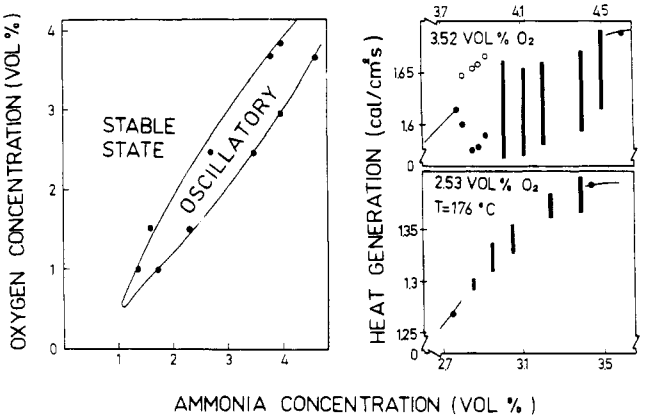

Figure 8. Bifurcation map and diagrams obtained at 176 °C.

by hysteresis. At 2.53% O_2 the behavior at both boundaries is characterized by bursts of periodic behavior on an otherwise stable state (Figure 9). The length of the fast oscillatory phase diminishes and the separation of two bursts increases as the boundary is approached. Inside the oscillatory domain the behavior is simple at high frequency. The sequence at 3.52% O_2 shows bifurcation from simple low-frequency oscillations to stable state at the lower boundary. The bifurcation is hard, as is evident from the diagram in Figure 8, and the period grows as the boundary is approached. A similar hard long-period bifurcation from an apparently aperiodic state (4.5% NH_3) occurs at the upper boundary. In-between high- and low-frequency aperiodic states are observed:

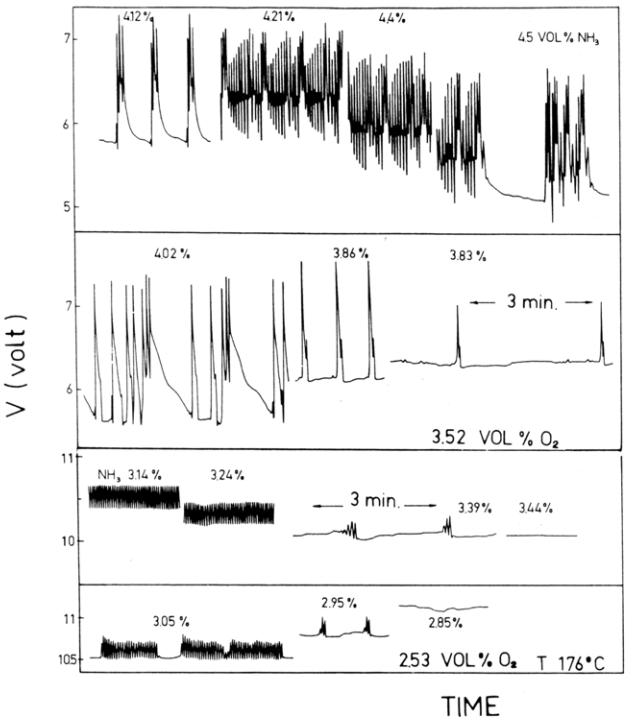

Figure 9. Sequences of time traces that correspond to the bifurcation diagrams in Figure 8.

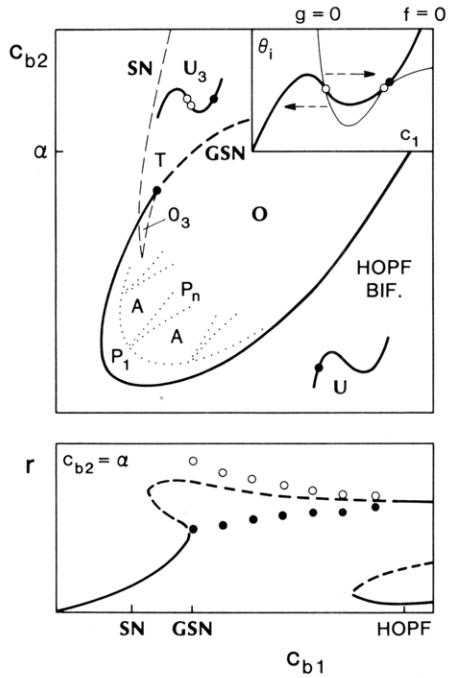

Figure 10. (Top) Schematic bifurcation map that accounts for Figure 1. The Hopf (solid) and saddle-node (broken) lines divide the map into regions of characteristic behavior. The insert shows the curves $f = 0$ and $g = 0$ of the GSN phase plane. (Bottom) Characteristic bifurcation diagram; it also shows the inactive branch which is not accounted for in the map.

the former are intermittent in nature (4.21% and 4.4% NH_3; Figure 9).

The bifurcation set at 176 °C is probably an infinite-period global saddle node. Unlike the Hopf bifurcation, the hard bifurcations may occur from complex or even aperiodic states. The time traces at 176 °C show fast (3-s) and slow (1-min) oscillations. The latter grow indefinitely as the boundary is approached since the trajectory travels in the vicinity of a saddle node. This bifurcation occurs from periodic simple slow oscillations, from aperiodic oscillations, or by intermittent bursting behavior (Figure 9).

Discussion

Our analysis is aimed at determining the main features of the underlying kinetic model. Although the physicochemical mechanism cannot be elucidated from reaction rate measurements, we discriminate between classes of model by capitalizing on the stoichiometric location of the oscillatory domain and the time scales evident in this reaction. The mathematical features of the model can be determined from the nature of bifurcations to periodic solution. More information can be gained from the structure of the oscillatory domain and the bifurcation to complex and aperiodic solutions.

Although oscillations are common to catalytic oxidation reaction, they were usually observed in oxygen-rich environment when catalyzed by a noble metal and in fuel-rich mixtures when catalyzed by Ni and Cu. The existence of oscillations around the stoichiometric ratio suggests that they are induced by competition between the two reactants and that gas-phase concentrations (C_i) should be employed as the dynamic variables. A simple CSTR-type model that accounts for reactant and product mass transfer and subsequent reaction (r_i) is

$$a_v^{-1}\dot{C}_i = k_{c_i}(C_{b_i} - C_i) - r_i \equiv f_i \qquad (1)$$

We will need to specify the "reactor" volume in equilibrium with unit surface area (a_v). Isothermal oscillations may be admitted by such a model with autocatalytic kinetics and different mass-transfer coefficients (k_{c_i}) of the two reactants. The period of these oscillations, however, is $(k_c a_v)^{-1}$ in order of magnitudes. Since at steady state $k_{c_i}(C_{b_i} - C_i) = r_i$, then the period is approximated by $C_{b_i}/r_i a_v$. The term r_i/C_{b_i} is 5–10 cm/s for our data, and unreasonably high values of volume to surface rations $(1/a_v)$ are required in order to account for the 3–10-s oscillations.

A model that accounts for a detailed surface mechanism will predict a period that is similar to the turnover number; since adsorption capacity is 2×10^{-9} g mol/cm^2, then such a model will predict millisecond oscillations. We are led to conclude, therefore, that the oscillations' long period is due to a slow surface modification, like surface oxidation on poisoning. A model with widely different time scales, a fast reaction, and a slow surface modification may account for the observed relaxation oscillations if the fast reaction admits multiple solutions in a range of surface modifications. The model may account for the domain of oscillations if the required bistability is attained around the stoichiometric ratio.

We may choose the reactant concentrations as the fast dynamic variables (eq 1) and the fraction of inactive surface area (θ) as the slow one. The latter equation may be written in the general form

$$\dot{\theta} = k_i g(C_1, C_2, \theta) \qquad (2)$$

The two reactant balances may be reduced to one dynamic equation when $r_2/r_1 = \nu$, a stoichiometric ratio, and $k_{c_1} = k_{c_2}$. We find then a linear relation between C_1 and C_2 and need to consider only two differential equations. For relaxation oscillations we are interested only in the shape of the curve of slow motion along $f_1 = f_2 = 0$ and we can find a dependence C_2 (C_1) under a much less restrictive assumption. We assume that two differential equations are sufficient to describe the system. We are now ready to specify the shapes of $f(C_1,\theta) = f_1(C_1, C_2(C_1),\theta) = 0$ and $g = 0$ that will admit the observed bifurcations at 160 °C.

At low reactant concentrations the oscillatory domain is bounded by the Hopf bifurcation points. At a high oxygen concentration the oscillations appear, with decreasing ammonia concentration, by a Hopf bifurcation and disappear via a global-saddle-node bifurcation. We have rejected the interpretation of a steep Hopf bifurcation since at 176 °C that boundary is clearly a global saddle node. Figure 10 (bottom) shows the stable and unstable branches of a schematic bifurcation diagram with these features. It also includes the inactive branch. We search therefore for a model that accounts for the transition between this diagram and one with two Hopf points. Systems with widely separated

time scales may indeed explain a boundary that changes from a Hopf bifurcation to a global saddle node. The details are described by Sheintuch and Luss;[6] Figures 5, 10, and 11 in ref 6 show typical phase planes and a bifurcation map of a specific model. We use that information in interpreting the NH_3 oxidation map.

Figure 10 (top) shows a qualitative bifurcation map that explains Figure 1. The Hopf and saddle-node bifurcation sets are denoted by continuous and broken lines, respectively; the two are tangent at point T, which separates each set to an observable (thick line) and an unobservable (thin line). Together they separate the plane into regions with the following phase planes: a unique state (U), a stable state coexisting with two unstable ones (U_3), and a limit cycle surrounding one (O) of three (O_3) states. The phase plane that corresponds to the global-saddle-node (GSN) boundary, shown in the inset, specifies the form of $f = 0$ and $g = 0$ null curves. The other phase planes are obtained by perturbations from it; the $f = 0$ line and the location of the steady states which are shown in Figure 10 are sufficient to determine the motion. Crossing the GSN, for example, introduces two steady states in the limit cycle path and destroys it. The Hopf line is crossed when a steady state moves through an extremum point of $f = 0$.

A possible qualitative model for the bifurcation map should have therefore the properties shown in Figure 10 (insert). A mechanistic model that obeys these specifications was suggested in ref 6 to account for observations of Hopf and global-saddle-node bifurcations during CO oxidation in excess oxygen. A Langmuir-Hinshelwood rate expression was employed there to obtain the multivalued $f = 0$ curve.

The skeleton two-variable model described above cannot account, of course, for complex oscillations. Furthermore, even our interpretation of the structure of the oscillatory domain is based on the analysis of difference equations and several numerical examples of ordinary differential equations. Mapping of the behavior of the simple circle map[20] $\theta_{n+1} = \theta_n + \Omega - (k/2\pi) \sin 2\pi\theta_n$, in the k-Ω plane, shows tongues of frequency-locked states interdispersed within quasiperiodic or chaotic states. On the basis of this result and our observations we draw schematically (dotted line, Figure 10) the boundaries of simple periodic and quasiperiodic behaviors and several frequency-locked tongues. There are an infinite number of these, and they may be terminated at the boundary of chaotic behavior. All three types of scenarios leading to chaos exist in the evolution of the circle map.

(20) Mackay, R. S.; Tresser, C. *Physica D (Amsterdam)* **1986**, *19D*, 206-237.

Concluding Remarks

This work demonstrates the advantages of applying recent mathematical studies of dynamical systems to the design and analysis of experimental results. The discussion shows that the most systematic study of dynamical systems is to map behavior in the parameter plane, instead of finding just a set of operating conditions corresponding to different phase-plane behavior. Obviously a map in a three-parameter space could be even more discriminatory for modeling purposes, but its finding requires a significant experimental effort.

The experimentation time required for drawing a bifurcation map increases with the characteristic period of the oscillation and with the degree of resolution required. Poor reproducibility of experiments reduces the resolution. The understanding of the B-Z and other liquid-phase reactions led to high degree of reproducibility in open systems and enabled a detailed mapping. Maselko and Swinney[14] recently mapped the nature of complex oscillations in the B-Z reaction. These oscillations are characterized by a mixture of small and large peaks at a ratio that varies in a fractal nature as a parameter is varied: between any two complex periodic states there exist other periodic solutions which are a mixture of the adjacent states. Catalytic oscillations are usually slow (minutes to hours) and are accompanied by a certain degree of irreproducibility due to the changing nature of the catalytic surface. Ammonia oxidation is exceptional in showing fast oscillation and relatively good reproducibility. That enabled a detailed mapping of bifurcations to periodicity in the parameter plane and of shape bifurcations in one parametric dimension. We showed that the richness of behavior in this, and presumably other, catalytic reactions is comparable to that of the B-Z reaction or of hydrodynamic systems.

This paper demonstrates that when the system is characterized by widely different time scales, a simple qualitative model may be developed from knowledge of the observed bifurcations to periodic behavior. This identification gives physical insight into the qualitative features of the balances $f = 0$ and $g = 0$. A similar approach for prediction of shape bifurcations is still lacking. Such modeling may be possible when the system shows a mixture of two kinds of oscillations (e.g., large and small; Figure 7); that is the subject of our current investigation.

Acknowledgment. This work was supported by the U.S.-Israel Binational Science Foundation. Data acquisition and analysis (Figures 4 and 6) were performed by Moshe Avihai.

Registry No. NH_3, 7664-41-7; Pt, 7440-06-4.

Thermodynamics of Hydrogen-Isotope-Exchange Reactions. 5. Determination of K and $\Delta S°$ for the Reaction $OD^-(daq) + HS^-(aq) \rightleftharpoons OH^-(aq) + DS^-(daq)$

On-Kok Chang and Peter A. Rock*

Department of Chemistry, University of California, Davis, Davis, California 95616 *(Received: April 27, 1987; In Final Form: January 8, 1988)*

This paper reports our results for the experimental determination of the equilibrium constant and its temperature dependence for the solution-phase hydrogen-isotope-exchange reaction $OD^-(daq) + HS^-(aq) \rightleftharpoons OH^-(aq) + DS^-(daq)$. The results were obtained from measurements on electrochemical double cells of the type $Pt(s)|D_2(g)|Na_2S(daq)|HgS(s)|Hg(l)|HgS(s)|Na_2S(aq)|H_2(g)|Pt(s)$ and analogous cells involving silver sulfide-silver electrodes in place of the mercuric sulfide-mercury electrodes. The experimental value of the equilibrium constant at 25.0 °C for the reaction is $K = 0.534 \pm 0.011$; the experimental value of the standard entropy change at 25.0 °C for the reaction is $\Delta S° = 7.0 \pm 1.8$ J·K^{-1}.

Introduction

This paper reports part of a continuing investigation of the thermodynamics of hydrogen-isotope-exchange reactions[1-4] directed toward (1) providing experimental data to test the statistical thermodynamic theory of isotope-exchange reactions; and (2)

(1) Silvester, L. F.; Kim, J. J.; Rock, P. A. *J. Chem. Phys.* **1972**, *56*, 1863.
(2) Rock, P. A. *ACS Symp. Ser.* **1975**, *11*, 131.

* Author to whom correspondence should be addressed.

0022-3654/88/2092-3411$01.50/0